Published in final edited form as:
Nat Biotechnol. 2017 February ; 35(2): 164–172. doi:10.1038/nbt.3770.

Influence of node abundance on signaling network state and dynamics analyzed by mass cytometry

Xiao-Kang Lun[1,2], **Vito RT Zanotelli**[1,3], **James D Wade**[1,4], **Denis Schapiro**[1,3], **Marco Tognetti**[1,2,5], **Nadine Dobberstein**[1], and **Bernd Bodenmiller**[1]

[1]Institute of Molecular Life Sciences, University of Zürich, Zürich, Switzerland [2]Molecular Life Science Ph.D. Program, Life Science Zürich Graduate School, ETH Zürich and University of Zürich, Zürich, Switzerland [3]Systems Biology Ph.D. Program, Life Science Zürich Graduate School, ETH Zürich and University of Zürich, Zürich, Switzerland [4]Wallace H. Coulter Department of Biomedical Engineering, Georgia Institute of Technology and Emory University, Atlanta, Georgia, United States of America [5]Institute of Biochemistry, ETH Zürich, Zürich, Switzerland

Abstract

Signaling networks are key regulators of cellular function. Although the concentrations of signaling proteins are perturbed in disease states, such as cancer, and are modulated by drug therapies, our understanding of how such changes shape the properties of signaling networks is limited. Here we couple mass cytometry-based single-cell analysis with overexpression of tagged signaling proteins to study the dependence of signaling relationships and dynamics on protein node abundance. Focusing on the epidermal growth factor receptor (EGFR) signaling network in HEK293T cells, we analyze 20 signaling proteins during a one hour EGF stimulation time course using a panel of 35 antibodies. Data analysis with BP-R^2, a measure that quantifies complex signaling relationships, reveals abundance-dependent network states and identifies novel signaling relationships. Further, we show that upstream signaling proteins have abundance-dependent effects on downstream signaling dynamics. Our approach elucidates the influence of node abundance on signal transduction networks and will further our understanding of signaling in health and disease.

Signaling networks are at the core of cellular information processing and transform external signals into cellular responses. Signals are transduced by modulating enzymatic activities mainly via protein phosphorylation, and cells implement sophisticated mechanisms, such as

Correspondence should be addressed to B.B. (bernd.bodenmiller@imls.uzh.ch).

Accession Codes

All data and working illustrations are available on Cytobank.org under the project 725. The BP-R^2-based analysis is provided as Supplementary Software and the GitHub repository https://github.com/BodenmillerGroup/Adnet.

Author Contributions

X.K.L. and B.B. conceived and designed the experiments. X.K.L., M.T. and N.D. performed experiments. V.Z., J.D.W., X.K.L. and D.S. performed data analysis. X.K.L. and B.B. wrote the manuscript. All authors commented on and edited the final version of the paper.

Competing Financial Interest

The authors declare no competing financial interest.

Europe PMC Funders Author Manuscripts

feedback loops, pathway crosstalk, and differential enzyme localization, to integrate signals and drive cellular processes and physiological outputs. The abundance of individual signaling pathway components (nodes) is central to the activity and output of a signaling network1. Changes in node abundance are tightly regulated and control biological programs such as stem cell differentiation and embryogenesis2. Abundance deregulation of particular signaling network nodes via genomic, transcriptional, or post-transcriptional regulatory defects3–5 underlies human diseases, the prime example being cancer6. Copy number alterations of genes encoding critical proteins7–9, independent of mutations that constitutively change enzymatic activity10, drive progression of many cancer types. Genomic instability in cancer cells causes abnormally broad distributions of signaling protein abundances in a given tumor11, yet the consequences of the protein abundance levels on signaling properties is poorly understood limiting our ability to rationally design therapies.

The epidermal growth factor receptor (EGFR) signaling network is affected by gene copy number alterations that deregulate protein abundances (e.g., of EGFR, HER2, ERK and AKT) in a number of cancer types7–9. EGFR signaling controls cell growth, motility, survival, differentiation, and metabolism12. Many drugs target the activity of the EGFR signaling network13,14. The receptor tyrosine kinase (RTK) function of EGFR is activated by its dimerization upon ligand binding. EGFR auto-phosphorylation recruits adaptor proteins that typically activate the MAPK/ERK and AKT signaling pathways. The MAPK/ERK branch activates the GTPase RAS, which triggers a kinase phosphorylation cascade consisting of RAF, MEK, ERK, and p90RSK. The output of the MAPK/ERK branch is transcription of genes regulating growth and division15,16. Signal transduction through the AKT branch starts by PI3K activation, producing PIP3, which recruits AKT and PDK1 to the plasma membrane. PDK1 phosphorylates AKT15,17, which mediates signaling through the mTORC1 complex to modulate translation via p70S6K and 4EBP117. Other AKT targets are GSK3β, PRAS40, and TSC2. The AKT pathway controls cell survival, proliferation, and migration17. STAT proteins and the PKC pathway can also be activated by EGFR-mediated signaling18,19. EGFR signaling involves crosstalk and feedback loops both internally (e.g., active ERK attenuates upstream RAF or MEK signaling via negative feedback)15 and with other signaling pathways (e.g., WNT and TGF-β pathways)20,21.

Classically, two approaches are used to characterize the effect of proteins on signal transduction. The first approach analyzes cell populations. Here, western blotting, mass spectrometry, RNA-microarrays, and synthetic lethality screens are used to identify signaling relationships22–24. Protein-protein interaction analyses are used to determine which proteins in a network directly interact23,25. Population-based methods yield a comprehensive view of signaling but are difficult to use in analysis of protein abundance dependencies due to inherent limitations: Proteins must be expressed at different abundances or cells must be sorted to yield a non-continuous abundance titration. Such methods result in a large number of samples and cell-to-cell protein abundance variations within each sample remain masked. The second approach studies signaling relationships in single cells. Here fluorescence microscopy and flow cytometry (FACS) are used with a variety of assays, including proximity ligation assay (PLA)26 or fluorescence resonance energy transfer

(FRET)27. These approaches allow study of signaling relationships and dynamics through time and space; however, only a few signaling nodes can be measured simultaneously.

A recently developed single-cell analysis technology, called mass cytometry, allows for the simultaneous measurement of over 40 signaling nodes in single cells using metal-isotope tagged antibodies28,29. This capability makes mass cytometry uniquely suited to comprehensively query the function of nodes in signaling networks within heterogeneous cell populations. Mass cytometry is quantitative and, in combination with mass-tag cellular barcoding (MCB), a powerful screening tool28. Algorithms to analyze multiplexed single-cell mass cytometry data allow quantification of signaling relationships, therefore helping to decipher the highly complex network behaviors that operate even in simple biological systems30.

Here, we coupled protein overexpression with mass cytometry to measure the effect of varying node abundance on the activation state and signaling relationships of an unstimulated EGFR signaling network, as well as the signaling dynamics of the network in response to EGF stimulation. We exploited the finding that transient protein overexpression in a cell population typically produces a continuous abundance range of the target protein over four orders of magnitude. We overexpressed 20 central EGFR signaling network proteins individually in human embryonic kidney (HEK) 293T cells, sampled during an EGF stimulation time course over 60 minutes totaling 360 conditions. An average of 11,000 cells per condition was analyzed with a panel of 35 antibodies to provide a comprehensive single-cell proteomic EGFR network analysis. To identify signaling relationships in this dataset, we developed a statistical measure that we call 'binned pseudo R-squared' (BP-R^2) that recapitulated known signaling relationships and identified relationships that were –to the best of our knowledge- not described previously. Thus, our experimental and computational approach enables study of how the strength and dynamics of signal transduction are tuned by node abundances.

Results

Analyzing continuous protein abundance dependencies

To systematically identify and characterize protein abundance-dependent signaling relationships, dynamics, and network activation states, we exploited the variation and large dynamic range of protein abundance induced by transient transfection and used mass cytometry to quantify the abundance of the transfected protein of interest (POI) in conjunction with comprehensive signaling network readouts in single cells. We cloned POIs genes into vectors containing a cytomegalovirus (CMV) promoter and a GFP-tag sequence31 to transiently overexpress GFP-tagged POIs in HEK293T cells (Fig. 1a). The tagged protein abundance was measured by mass cytometry using an anti-GFP antibody (Fig. 1a). Ordering the measured cells based on the GFP signal provided a continuous POI titration (Fig. 1b). Typically, not all cells were transfected, yielding an internal control for every experiment. To measure the single-cell EGFR signaling network states, we designed and validated a panel of 35 antibodies that mostly detect phosphorylation sites on signaling proteins (Supplementary Tables 1-3). These data were used to determine the abundance dependencies of network activation state and signaling dynamics (Fig. 1b).

To validate our system we confirmed that, first, the GFP tag was reliably detected by mass cytometry (Supplementary Fig. 1); second, the GFP tag did not affect the localization and activity of the POI (Supplementary Fig. 2, 3, Supplementary Table 4, Supplementary File 1); third, POI expression levels were linearly related to GFP abundance, validating GFP as readout of the total POI abundance (Supplementary Fig. 4a, c); fourth, POI overexpression for 18 hours (i.e., the time point of our experiments) did not alter the underlying network structure (Supplementary Fig. 4b, c); fifth, the antibody-based GFP quantification by mass cytometry was comparable to FACS (Supplementary Fig. 5); sixth, the cell culture media and cell detachment did not alter signaling processing in the EGFR network (Supplementary Fig. 6, 7); and, seventh, the levels of the GFP-tagged POIs were stable during the 1-hour EGF stimulation time course (Supplementary Fig. 8, Supplementary Video 1). We also found that the method is robust and highly reproducible as evidenced by the high concordance between the three individual experiment replicates (Supplementary Fig. 9, Supplementary File 2).

$KRAS^{G12V}$ and $MEK1^{DD}$ abundance effect on signaling

We first studied a well-known signaling circuit: Constitutively active mutants of KRAS and MEK1 ($KRAS^{G12V}$ and $MEK1^{DD}$) lead to ERK phosphorylation and activate components downstream in the MAPK/ERK pathway. As expected, we found that overexpression of $KRAS^{G12V}$-GFP or $MEK1^{DD}$-GFP increased phosphorylation on Thr202 and Tyr204 of ERK1/2 (Fig. 2a). Our approach also elucidated the abundance-dependent effects on these signaling relationships: The relationship between $KRAS^{G12V}$-GFP and p-ERK1/2 was bow-like as high levels of $KRAS^{G12V}$-GFP corresponded to reduced phosphorylation of ERK1/2. By contrast, the $MEK1^{DD}$-GFP abundance relationship with p-ERK1/2 was monotonic as p-ERK1/2 increased with $MEK1^{DD}$-GFP expression (Fig. 2a). These results verified the oncogenic activation of p-ERK1/2 induced by $KRAS^{G12V}$ and $MEK1^{DD}$.

Next, we analyzed the impact of $KRAS^{G12V}$-GFP and $MEK1^{DD}$-GFP abundance on all measured phosphorylation sites. We divided the measured cells into 10 bins according to the GFP signals and plotted the bin medians (Fig. 2b, Supplementary Fig. 9b-e). This analysis revealed that the phosphorylation site abundances on ERK1/2 and its direct downstream target Ser380 of p90RSK had similar relationships to the abundances of $KRAS^{G12V}$-GFP or $MEK1^{DD}$-GFP. Phosphorylation of AKT on Ser473 and its direct target Ser9 of GSK3β also had parallel trends and showed reduced levels when the MAPK/ERK signal peaked, suggesting inter-pathway regulation. We also observed increased JNK phosphorylation on Thr183/Tyr185 induced by the $KRAS^{G12V}$ mutant (Fig. 2b) as reported previously32. This shows that our approach recapitulates known signaling relationships and identifies abundance-determined signaling responses.

We then systematically evaluated signaling relationships between all pairs of measured markers modulated by $KRAS^{G12V}$-GFP or $MEK1^{DD}$-GFP overexpression. We exploited the fact that overexpression of one protein increases signaling (i.e., phosphorylation levels) and thus expands the dynamic range of many measured markers (Fig. 2c). This enabled the use of correlation analysis to distinguish signaling relationships (high correlation) from biological and technical noise (low correlation). For example, overexpression of $KRAS^{G12V}$-

GFP resulted in an increased Spearman correlation between p-ERK1/2 and p-p90RSK compared to control (Fig. 2c), whereas ERK-independent phosphorylation sites, such as Tyr551 of BTK/ITK, showed low correlation with p-ERK1/2 levels in both control and overexpression conditions (Fig. 2d).

Identifying changes in pairwise Spearman correlations for all measured markers in the $KRAS^{G12V}$-GFP and $MEK1^{DD}$-GFP overexpression data compared to the FLAG-GFP control enabled systematic analysis of signaling relationship patterns (Fig. 2e, f). Phosphorylation levels of proteins in the MAPK/ERK pathways showed strong increases in correlation, and pathway members clustered together (Fig. 2e, f, green squares). We also observed that phosphorylations of MAPK/p38 pathway members and STAT proteins (STAT1 and STAT5) were increasingly correlated with levels of MAPK/ERK pathway members as MEK^{DD}-GFP levels increased (Fig. 2f, purple rectangle), indicating crosstalk between MAPK and STAT pathways. These results reveal relationships among many measured markers and show that increases in correlation reflect pathways and grouped biological processes.

Automated analysis of abundance-induced signaling

Spearman correlation analysis can uncover strictly monotonic relationships between phosphorylation levels on signaling proteins; however, protein abundance-dependent signaling responses can be complex (Fig. 2a, see $KRAS^{G12V}$). We therefore developed a density-independent measure termed 'binned pseudo R-squared' (BP-R^2) to quantify the strengths of relationships between the abundance of a POI and measured phosphorylation sites. BP-R^2 creates 10 bins across the POI-GFP expression range and calculates the relationship strength considering bin medians and the global mean (Supplementary Fig. 10a, b, Methods, Supplementary Software). Using the BP-R^2 values for all negative controls, a cutoff for strong signaling relationships was determined (Supplementary Fig. 10c). Benchmarking BP-R^2 in identifying strong signaling relationships from the overexpression datasets showed that BP-R^2 outperformed methods often used for this task30,33 (Supplementary Fig. 11a, b). The strong relationships identified by BP-R^2 were plotted in a two-dimensional layout guided by canonical pathways (Fig. 2g, h). The directionality of measured signaling relationships was determined by Spearman correlation of the bin medians (Supplementary Fig. 10b, Methods). A positive correlation indicates that cells show generally increasing marker levels and a negative correlation indicates generally decreasing marker levels as POI-GFP levels increase.

Analysis of $KRAS^{G12V}$-GFP and $MEK1^{DD}$-GFP overexpression versus all measured markers using BP-R^2 revealed strong, positively correlated relationships of MEK^{DD}-GFP to downstream MAPK/ERK pathway nodes. $KRAS^{G12V}$-GFP levels, although also positively correlated with MAPK/ERK nodes, exhibited the same, but weaker relationships (Fig. 2a, b, g, h). Together, these results suggest that feedback regulation of upstream MAPK nodes differs between the studied mutants. Additionally, this network view revealed that $MEK1^{DD}$-GFP abundance had a strong positive impact on nodes in the MAPK/p38 pathway; the previously observed $KRAS^{G12V}$-induced phosphorylation of JNK32 was dependent on $KRAS^{G12V}$ abundance (Fig. 2g, h). These results show that overexpression of signaling

proteins, in conjunction with BP-R^2 and correlation analysis, identifies known relationships and is a valid platform for discovery of signaling relationships in a comprehensive and abundance-dependent manner.

Node abundance dependency analyses of the EGFR network

To study the node abundance dependency of signaling relationships and dynamics in the EGFR signaling network, we overexpressed 20 EGFR-related signaling proteins individually in HEK293T cells (Table 1). Each of the 20 GFP-tagged POIs was validated in previous studies (Supplementary Table 5) and in our system (Supplementary Fig. 2, 3, Supplementary File 1). 18 hours after transfection, we treated cells with EGF and quantified signaling by mass cytometry over a 60-min time course. To exclude signaling relationships caused by channel-to-channel spillover, we applied a stringent experimental filter (Supplementary Fig. 12, Methods). The median marker intensities during the time course are shown in Supplementary Fig. 13a. Based on these data we performed two sets of analyses. In the first, we used BP-R^2 analysis and Spearman correlations to evaluate how the abundance of overexpressed proteins influenced phosphorylation at the measured sites (Fig. 3, Supplementary Fig. 13b and Supplementary Files 2-4). In the second, we examined how features of signaling dynamics depend on protein abundance (Fig. 4).

In the first analysis, strong and broad signaling responses to overexpression were identified for the upstream kinases PDK1-, GSK3β-, SRC-, and ASK1-GFP without EGF stimulation (Fig. 3. Overall, we identified 59 strong signaling relationships in the unstimulated conditions. Overexpression of many kinases induced strong and positively correlated signaling relationships with their own phosphorylation (Fig. 3, Supplementary File 4). Overexpression of CRAF-, KRAS-, p70S6K-GFP, and others only induced signaling responses upon EGF stimulation (Fig. 3). Notably, under stimulated conditions, KRAS-, CRAF-, and MEK1-GFP levels negatively correlated with phosphorylation levels of downstream kinases p-ERK1/2 and p-p90RSK (Fig. 3). Activating mutations in KRAS and CRAF (Fig. 2), but not protein overexpression alone, may activate oncogenic signaling.

To systematically assess signaling relationships identified by BP-R^2, we used the literature-based signaling network, SIGNOR34. For each relationship, we computed the shortest signed directed path length according to the SIGNOR network (Supplementary Table 6). We found that 76% of the strong relationships identified in the unstimulated conditions had paths with a maximum of three steps, highlighting that our approach identifies rather direct signaling relationships. Only 14 abundance-dependent relationships with four or more path steps were identified. Comparison of our strong signaling relationships with literature indicated that many EGF signaling connections that we identified were previously reported. We also propose many relationships that have—to our knowledge—not been previously reported, for example: p90RSK to PDK1 (Ser241), GSK3β to SHP2 (Tyr580), JNK1 to MAPKAPK2 (Thr334), p110α to MKK3 (Ser189), p110α to MKK6 (Ser207), ASK1 to PDK1 (Ser241), ASK1 to GSK3β (Ser9), and ASK1 to AMPKα (Thr172) (Table 2).

Phosphorylation levels of many members of the MAPK/ERK pathways showed complex relationships (i.e., measured phosphorylation levels varied over the analyzed POI-GFP range and the relationships did not fit linear, sigmoidal, or quadratic models) with levels of POI-

Europe PMC Funders Author Manuscripts

GFPs upon EGF stimulation. These relationships can be explained by abundance-dependent modulation of the signaling dynamics in response to EGF. Thus, in the second set of analyses we examined how signaling dynamics, as quantified by amplitude and peak-time, depended on abundance of an overexpressed protein (Fig. 4). In order to view signaling trajectories as functions of protein abundance, we binned the POI-GFP levels into 10 bins (Fig. 4a, Supplementary File 2). This allowed tracing the signaling trajectories of cells with similar protein overexpression levels (i.e., those in the same bin) over the EGF stimulation time course (Fig. 4b, Supplementary File 5). Strong and robust changes in signaling amplitudes (Fig. 4c-i) and peak-times (Supplementary Fig. 14) were found. Notably, the maximum amplitudes were independent of the overexpression range of a given POI (Supplementary Fig. 15).

We found that high CRAF-GFP and KRAS-GFP abundance strongly reduced signaling amplitudes of p-ERK1/2 and p-p90RSK (Fig. 4c, d, i), whereas high abundance of MEK1-GFP strongly reduced amplitudes and delayed peak-times for p-p90RSK (Fig. 4i, Supplementary Fig. 14). Overexpression of ERK2-GFP led to complex abundance-dependent responses of p-p90RSK and p-ERK1/2 after EGF stimulation (Fig. 4e-h). p-ERK1/2 amplitudes increased and peak-times delayed as a function of ERK2-GFP abundance level (Fig. 4g-i, Supplementary Fig. 14). Intermediate abundance levels of ERK2-GFP also delayed the p-p90RSK peak-times relative to low ERK2-GFP abundance, whereas cells with high ERK2-GFP levels exhibited minimal p-p90RSK signaling dynamics (Fig. 4e, f, i, Supplementary Fig. 14). Overexpression of p90RSK-GFP modulated the signaling amplitude of its potential crosstalk phosphorylation site, Ser241 of PDK1, in an abundance-dependent manner, and increasing expression of p90RSK increased p-PDK1 amplitudes (Fig. 4i). Thus, we observed abundance-dependent signaling dynamics across the range of overexpression levels. Overexpression of upstream signaling proteins (KRAS-, CRAF-, MEK1-, and ERK2-GFP) in the MAPK/ERK pathway led to reduced signaling amplitudes and delayed peak-times of their downstream targets. These observations show that our approach can quantify the role of protein abundance in determining the dynamic signaling response to an extracellular stimulation.

Discussion

Here we present an approach coupling transient overexpression with mass cytometry-based single-cell measurements to characterize signaling network activation states and signaling dynamics over a quasi-continuous, high dynamic range of protein abundance. To highlight the utility of our approach, we present a comprehensive single-cell proteomic analysis of the EGFR network that enabled an analysis of abundance-dependent effects of signaling proteins on state and dynamics of the signaling network. We evaluated the effects of overexpressing 20 EGFR network key nodes with a 60-minute EGF stimulation time course. In each of the 360 conditions, we measured the effect of a POI over a four order of magnitude abundance range on 35 markers by mass cytometry providing a unique and valuable quantitative single-cell resource of abundance dependencies of EGFR signaling.

Previously, the heterogeneity of protein levels after transient transfection was considered problematic. Here, we took advantage of this cell-to-cell variation as it results in a

continuous titration of protein abundance over four orders of magnitude. Untransfected cells also provided an internal control for each experiment. We used the multiplexing capabilities of mass cytometry to characterize abundance dependencies of signaling network state and dynamics. Applied to the EGFR signaling network, our approach recapitulated known relationships, suggested previously not described ones, and revealed the intricate modulation of signal amplitudes and peak-times as functions of continuous protein abundance.

Our approach contributes to the understanding of signaling on several levels. First, the approach can be used to study uncharacterized proteins and to suggest additional roles to characterized ones. Second, we were able to directly relate POI abundance with the comprehensive analysis of signaling dynamics in response to stimulation. Such analyses are necessary for understanding of differential signal processing in identical cell types and in disease states characterized by heterogeneity in protein expression such as cancer. Third, the overexpression yields a large dynamic range of signaling activity and can reveal signaling relationships masked by stochastic processes and technical noise under otherwise similar conditions, facilitating the computational analysis of signaling relationships. Fourth, we present a metric termed BP-R^2, which allows the quantification of the strengths of arbitrary shaped signaling relationships. BP-R^2 was superior to state-of-the-art methods for analysis of our dataset. Fifth, and finally, we were able to infer protein abundance-dependent signaling kinetics from single-cell snapshot data.

Our approach recapitulated known oncogenic signaling behaviors induced by the constitutively active mutants $KRAS^{G12V}$ and $MEK1^{DD}$ and identified novel abundance-dependent signaling relationships. For example, p-ERK1/2 was attenuated in cells with highly overexpressed $KRAS^{G12V}$-GFP, potentially due to negative feedback loops or senescence35. Overexpression of the wild-type KRAS-GFP and MEK1-GFP did not induce downstream signaling activation, suggesting that mutations on KRAS or MEK1 are the main drivers of oncogenic signaling. Further, our approach allows study of abundance-dependent signaling dynamics. In the MAPK/ERK pathway, high abundance of upstream signaling mediators KRAS, CRAF, MEK1, or ERK2 reduced amplitudes and delayed peak-times of downstream phosphorylation sites. One possible explanation is that the signal transduction is determined by the competition between active and inactive forms of a signaling protein for substrates. Overexpression increases the total abundance but may reduce the percentage of the active form.

KRAS amplification has been identified in many cancer types. Amplification, however, is not correlated with the phosphorylation of ERK1/236. Rather, *KRAS* amplification mediates resistance to inhibitors targeting growth pathway related kinases, including EGFR, MET and MEK1/2; KRAS knockdown diminishes the drug resistance37–39. Our results indicate that due to reduced downstream signaling amplitudes in response to EGF stimulation, the dependency of cells on the MAPK/ERK pathway may decrease upon KRAS overexpression, suggesting a mechanism for cancer cell resistance to inhibitors.

Comparing the identified strong signaling relationships with those in the SIGNOR database, we propose previously not described signaling relationships, e.g.: 1) Our data suggest that p90RSK potentially forms a positive feedback loop and activates the upstream signaling

protein PDK1. 2) GSK3β has been identified as a central signaling controller and has multiple substrates40; our results suggest that SHP2 is a potential direct or indirect target of GSK3β. 3) We also propose that JNK1 is a MAPKAPK2 activator. 4) PI3K and MKK3/6 are known to be regulated by RAC141; our results suggest PI3K activates MKK3/6 independently. 5) Recent studies indicate that ASK1 contributes in negative regulation of PDK1 through phosphorylation on Thr254 of PDK142; We observe ASK1 overexpression-induced PDK1 phosphorylation on Ser241, inducing PDK1 activity and downstream GSK3β phosphorylation on Ser9. 6) In addition to the known AMPK-mediated ASK1 activation43, our data indicates ASK1 activation of AMPKα via phosphorylation on Thr172. 7) We have also observed negative correlations between the abundance of p70S6K or PDK1 to the phosphorylation level of S6 (Ser235/Ser236), indicating overexpression-induced-negative feedback regulations.

Our method has several limitations. First, we do not measure the endogenous expression level of the POI. However, exogenous expression is linearly correlated with the total protein level (Supplementary Fig. 4a), validating GFP as readout of the total POI. Second, all results in mass cytometry rely on antibodies; for this work, all antibodies were thoroughly validated (Supplementary Table 3). Third, we do not measure the abundance range of the studied proteins in cancer cells, however, proteome studies of cancer cells and databases such as PaxDb11 indicate a range similar to those studied here. Fourth, high expression levels of a protein kinase may induce non-specific phosphorylation; however, our data allows choosing the analyzed expression range *in silico*, thus such effects can be excluded.

The approach described here provides a method to study how the abundance variance of signaling proteins in different tissues and cell lines results in distinct signaling behaviors. The application of our approach to synthetic biology, stem cell biology, developmental biology, and cancer-related processes, such as the epithelial-mesenchymal transition, will enable quantitative identification of key proteins and signaling determinants in cell differentiation at phenotypical switching points. We envision that determining which signaling relationships and thresholds enable diseased cells to overcome drug treatment will be a highly relevant application.

Supplementary Material

Refer to Web version on PubMed Central for supplementary material.

Acknowledgements

We would like to thank the Bodenmiller lab for support and fruitful discussions, the Lehner lab and the Mosimann lab for sharing equipment. We would especially like to thank Dr. A-C. Gingras, Lunenfeld-Tanenbaum Research Institute, for sharing the pDEST vectors used in this study. This work was supported by the Swiss National Science Foundation (SNSF) R'Equip grant 316030-139220, a SNSF Assistant Professorship grant PP00P3-144874, a Swiss Cancer League grant, the PhosphonetPPM SystemsX grant, and funding from the European Research Council (ERC) under the European Union's Seventh Framework Programme (FP/2007-2013) / ERC Grant Agreement n. 336921. The work of J.D.W. was supported by a National Science Foundation Graduate Research Fellowship under Grant No. DGE-1148903 and a Whitaker International Fellowship awarded by the Institute of International Education. The work of D. S. is supported by the Forschungskredit of the University of Zurich Fellowship.

References

1. Wolf-Yadlin A, et al. Effects of HER2 overexpression on cell signaling networks governing proliferation and migration. Mol Syst Biol. 2006; 2:54. [PubMed: 17016520]
2. De Los Angeles A, et al. Hallmarks of pluripotency. Nature. 2015; 525:469–478. [PubMed: 26399828]
3. Feinberg AP. Phenotypic plasticity and the epigenetics of human disease. Nature. 2007; 447:433–40. [PubMed: 17522677]
4. Bywater MJ, Pearson RB, McArthur GA, Hannan RD. Dysregulation of the basal RNA polymerase transcription apparatus in cancer. Nat Rev Cancer. 2013; 13:299–314. [PubMed: 23612459]
5. Silvera D, Formenti SC, Schneider RJ. Translational control in cancer. Nat Rev Cancer. 2010; 10:254–66. [PubMed: 20332778]
6. Santarius T, Shipley J, Brewer D, Stratton MR, Cooper CS. A census of amplified and overexpressed human cancer genes. Nat Rev Cancer. 2010; 10:59–64. [PubMed: 20029424]
7. Govindarajan B, et al. Overexpression of Akt converts radial growth melanoma to vertical growth melanoma. J Clin Invest. 2007; 117:719–29. [PubMed: 17318262]
8. Eralp Y, et al. MAPK overexpression is associated with anthracycline resistance and increased risk for recurrence in patients with triple-negative breast cancer. Ann Oncol. 2008; 19:669–74. [PubMed: 18006896]
9. Han T, et al. PTPN11/Shp2 Overexpression Enhances Liver Cancer Progression and Predicts Poor Prognosis of Patients. J Hepatol. 2015; doi: 10.1016/j.jhep.2015.03.036
10. Davies H, et al. Mutations of the BRAF gene in human cancer. Nature. 2002; 417:949–54. [PubMed: 12068308]
11. Wang M, Herrmann CJ, Simonovic M, Szklarczyk D, von Mering C. Version 4.0 of PaxDb: Protein abundance data, integrated across model organisms, tissues, and cell-lines. Proteomics. 2015; 15:3163–8. [PubMed: 25656970]
12. Citri A, Yarden Y. EGF-ERBB signalling: towards the systems level. Nat Rev Mol Cell Biol. 2006; 7:505–16. [PubMed: 16829981]
13. Tebbutt N, Pedersen MW, Johns TG. Targeting the ERBB family in cancer: couples therapy. Nat Rev Cancer. 2013; 13:663–73. [PubMed: 23949426]
14. Roberts PJ, Der CJ. Targeting the Raf-MEK-ERK mitogen-activated protein kinase cascade for the treatment of cancer. Oncogene. 2007; 26:3291–310. [PubMed: 17496923]
15. Mendoza MC, Er EE, Blenis J. The Ras-ERK and PI3K-mTOR pathways: cross-talk and compensation. Trends Biochem Sci. 2011; 36:320–8. [PubMed: 21531565]
16. Olayioye MA, Neve RM, Lane HA, Hynes NE. The ErbB signaling network: receptor heterodimerization in development and cancer. EMBO J. 2000; 19:3159–67. [PubMed: 10880430]
17. Manning BD, Cantley LC. AKT/PKB signaling: navigating downstream. Cell. 2007; 129:1261–74. [PubMed: 17604717]
18. Bowman T, Garcia R, Turkson J, Jove R. STATs in oncogenesis. Oncogene. 2000; 19:2474–88. [PubMed: 10851046]
19. Oliva JL, Griner EM, Kazanietz MG. PKC isozymes and diacylglycerol-regulated proteins as effectors of growth factor receptors. Growth Factors. 2005; 23:245–52. [PubMed: 16338787]
20. Kim D, Rath O, Kolch W, Cho K-H. A hidden oncogenic positive feedback loop caused by crosstalk between Wnt and ERK pathways. Oncogene. 2007; 26:4571–9. [PubMed: 17237813]
21. Massague J. Integration of Smad and MAPK pathways: a link and a linker revisited. Genes Dev. 2003; 17:2993–7. [PubMed: 14701870]
22. Zhang Y, et al. Time-resolved mass spectrometry of tyrosine phosphorylation sites in the epidermal growth factor receptor signaling network reveals dynamic modules. Mol Cell Proteomics. 2005; 4:1240–50. [PubMed: 15951569]
23. Kim SY, et al. AMP-activated protein kinase-α1 as an activating kinase of TGF-β-activated kinase 1 has a key role in inflammatory signals. Cell Death Dis. 2012; 3:e357.

24. Corcoran RB, et al. Synthetic lethal interaction of combined BCL-XL and MEK inhibition promotes tumor regressions in KRAS mutant cancer models. Cancer Cell. 2013; 23:121–8. [PubMed: 23245996]
25. Tewari M, et al. Systematic Interactome Mapping and Genetic Perturbation Analysis of a C. elegans TGF-β Signaling Network. Mol Cell. 2004; 13:469–482. [PubMed: 14992718]
26. Sundqvist A, et al. Specific interactions between Smad proteins and AP-1 components determine TGFβ-induced breast cancer cell invasion. Oncogene. 2013; 32:3606–15. [PubMed: 22926518]
27. Aoki K, et al. Stochastic ERK activation induced by noise and cell-to-cell propagation regulates cell density-dependent proliferation. Mol Cell. 2013; 52:529–40. [PubMed: 24140422]
28. Bodenmiller B, et al. Multiplexed mass cytometry profiling of cellular states perturbed by small-molecule regulators. Nat Biotechnol. 2012; 30:858–67. [PubMed: 22902532]
29. Bendall SC, et al. Single-cell mass cytometry of differential immune and drug responses across a human hematopoietic continuum. Science. 2011; 332:687–96. [PubMed: 21551058]
30. Krishnaswamy S, et al. Conditional density-based analysis of T cell signaling in single-cell data. Science. 2014; 1250689. doi: 10.1126/science.1250689
31. Couzens AL, et al. Protein interaction network of the mammalian Hippo pathway reveals mechanisms of kinase-phosphatase interactions. Sci Signal. 2013; 6:rs15. [PubMed: 24255178]
32. Zhou Y, et al. Chimeric mouse tumor models reveal differences in pathway activation between ERBB family- and KRAS-dependent lung adenocarcinomas. Nat Biotechnol. 2010; 28:71–8. [PubMed: 20023657]
33. Redell MS, et al. FACS analysis of Stat3/5 signaling reveals sensitivity to G-CSF and IL-6 as a significant prognostic factor in pediatric AML: a Children's Oncology Group report. Blood. 2013; 121:1083–93. [PubMed: 23243289]
34. Perfetto L, et al. SIGNOR: a database of causal relationships between biological entities. Nucleic Acids Res. 2016; 44:D548–54. [PubMed: 26467481]
35. Xu Y, Li N, Xiang R, Sun P. Emerging roles of the p38 MAPK and PI3K/AKT/mTOR pathways in oncogene-induced senescence. Trends Biochem Sci. 2014; 39:268–76. [PubMed: 24818748]
36. Rahman MT, et al. KRAS and MAPK1 gene amplification in type II ovarian carcinomas. Int J Mol Sci. 2013; 14:13748–62. [PubMed: 23820584]
37. Valtorta E, et al. KRAS gene amplification in colorectal cancer and impact on response to EGFR-targeted therapy. Int J cancer. 2013; 133:1259–65. [PubMed: 23404247]
38. Cepero V, et al. MET and KRAS gene amplification mediates acquired resistance to MET tyrosine kinase inhibitors. Cancer Res. 2010; 70:7580–90. [PubMed: 20841479]
39. Little AS, et al. Amplification of the driving oncogene, KRAS or BRAF, underpins acquired resistance to MEK1/2 inhibitors in colorectal cancer cells. Sci Signal. 2011; 4:ra17. [PubMed: 21447798]
40. Cohen P, Frame S. The renaissance of GSK3. Nat Rev Mol Cell Biol. 2001; 2:769–76. [PubMed: 11584304]
41. Shin I, Kim S, Song H, Kim H-RC, Moon A. H-Ras-specific activation of Rac-MKK3/6-p38 pathway: its critical role in invasion and migration of breast epithelial cells. J Biol Chem. 2005; 280:14675–83. [PubMed: 15677464]
42. Seong H-A, Jung H, Ichijo H, Ha H. Reciprocal negative regulation of PDK1 and ASK1 signaling by direct interaction and phosphorylation. J Biol Chem. 2010; 285:2397–414. [PubMed: 19920149]
43. Lee Y-K, Hwang J-T, Kwon DY, Surh Y-J, Park OJ. Induction of apoptosis by quercetin is mediated through AMPKalpha1/ASK1/p38 pathway. Cancer Lett. 2010; 292:228–36. [PubMed: 20083342]
44. Cardaci S, Filomeni G, Ciriolo MR. Redox implications of AMPK-mediated signal transduction beyond energetic clues. J Cell Sci. 2012; 125:2115–25. [PubMed: 22619229]
45. Rawlings JS, Rosler KM, Harrison DA. The JAK/STAT signaling pathway. J Cell Sci. 2004; 117:1281–3. [PubMed: 15020666]
46. Nyati MK, Morgan MA, Feng FY, Lawrence TS. Integration of EGFR inhibitors with radiochemotherapy. Nat Rev Cancer. 2006; 6:876–85. [PubMed: 17036041]

47. Mitra SK, Hanson DA, Schlaepfer DD. Focal adhesion kinase: in command and control of cell motility. Nat Rev Mol Cell Biol. 2005; 6:56–68. [PubMed: 15688067]
48. Hendriks RW, Yuvaraj S, Kil LP. Targeting Bruton's tyrosine kinase in B cell malignancies. Nat Rev Cancer. 2014; 14:219–32. [PubMed: 24658273]
49. Marin TM, et al. Shp2 negatively regulates growth in cardiomyocytes by controlling focal adhesion kinase/Src and mTOR pathways. Circ Res. 2008; 103:813–24. [PubMed: 18757826]
50. Wei ZZ, et al. Regulatory role of the JNK-STAT1/3 signaling in neuronal differentiation of cultured mouse embryonic stem cells. Cell Mol Neurobiol. 2014; 34:881–93. [PubMed: 24913968]

Europe PMC Funders Author Manuscripts

Europe PMC Funders Author Manuscripts

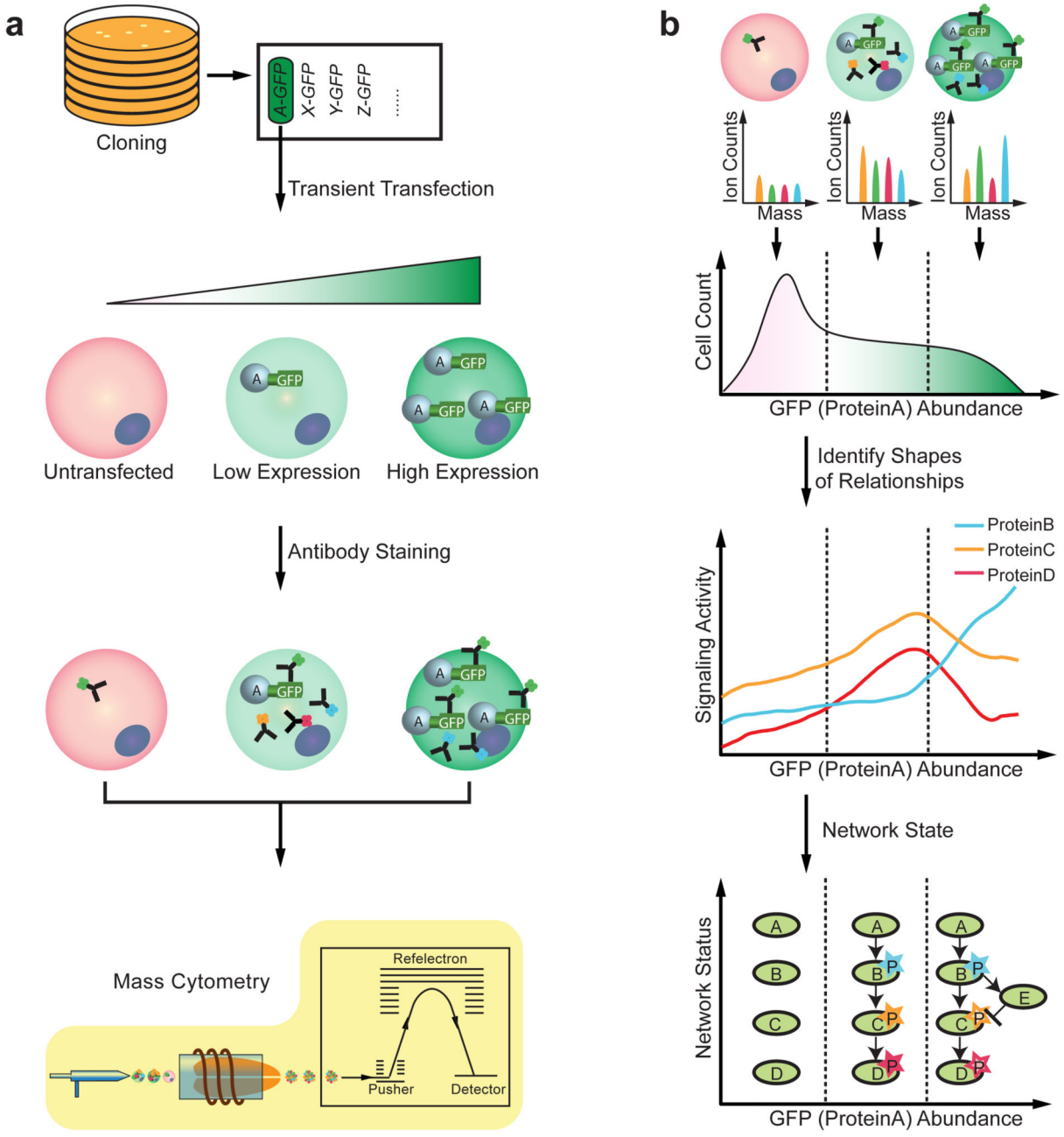

Figure 1.

Workflow of abundance-dependent network analysis. (**a**) Experimental workflow. Signaling POIs are cloned into vectors containing a CMV promoter and a GFP-tag sequence to transiently overexpress GFP-tagged POIs in HEK293T cells. We quantify anti-GFP antibody as readout of POI-GFP abundance, together with other 35 markers, by mass cytometry. (**b**) Data analysis workflow. Cells were ordered based on the GFP signal, providing a continuous POI titration, which was then coupled to other signaling markers to determine the abundance

dependencies of network activation state and signaling dynamics in the network after transfection. The network in the illustration does not represent an actual biological example.

Europe PMC Funders Author Manuscripts

Europe PMC Funders Author Manuscripts

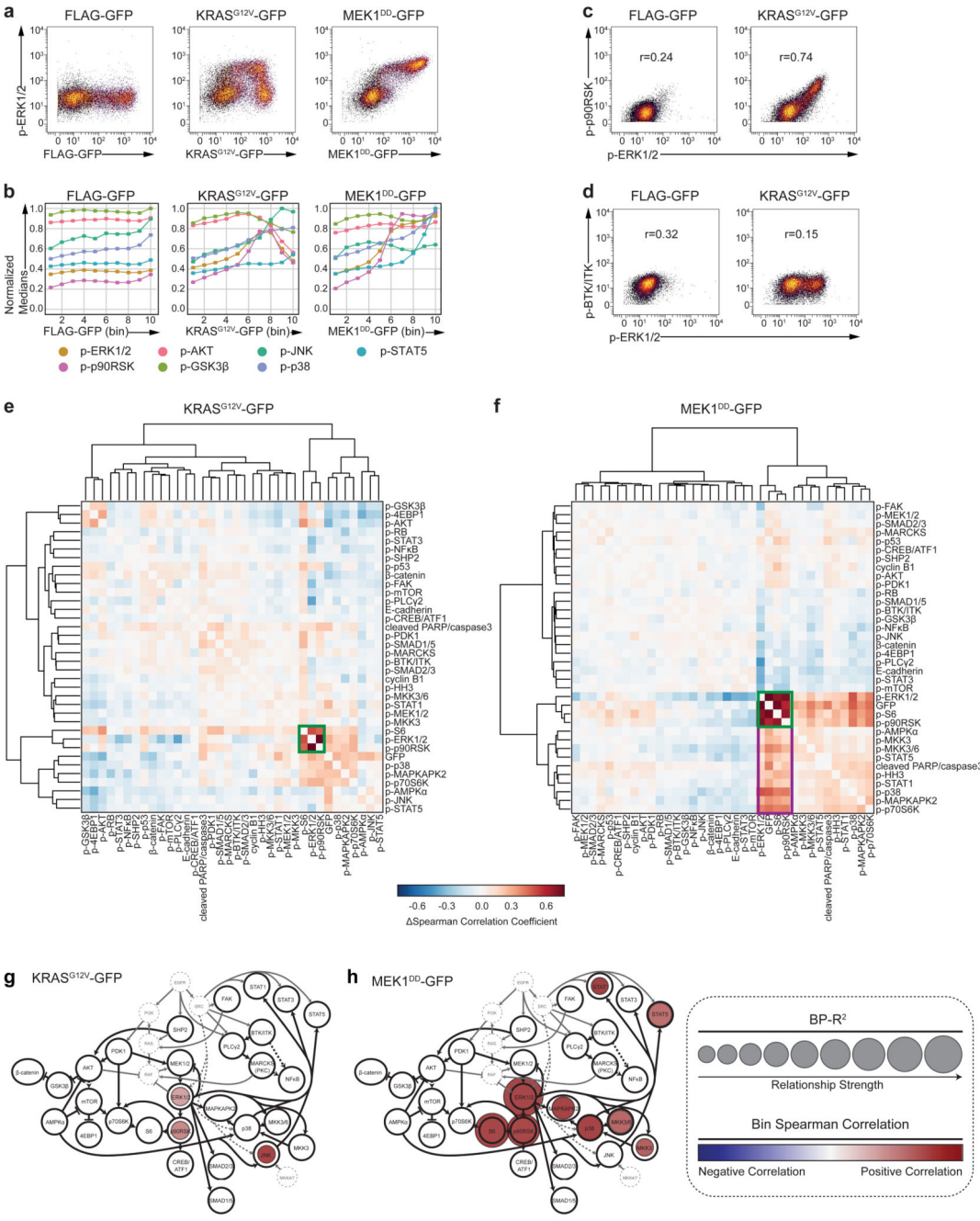

Figure 2.

MAPK/ERK pathway mutants induce oncogenic signaling. (**a**) Biaxial plots of GFP, representing the abundance of the overexpressed mutant POIs, versus abundance of phosphorylation on Thr202/Tyr204 on ERK1/2. Constitutively active KRAS^{G12V}-GFP shows a downregulation on Thr202/Tyr204 on ERK1/2 at the highest levels of KRAS^{G12V}-GFP. Constitutively active MEK1^{DD}-GFP directly phosphorylates Thr202/Tyr204 on ERK1/2, and the abundance of the POI-GFP is correlated with amount of ERK1/2 phosphorylated at these sites. The FLAG-GFP control does not affect ERK phosphorylation

sites. (**b**) The abundances of measured phosphorylation sites are plotted over the range of the $KRAS^{G12V}$-GFP and $MEK1^{DD}$-GFP expression. Phosphorylation sites of the same pathway (e.g., on ERK1/2 and p90RSK, AKT and GSK3β, or p38 and JNK) show similar trends. An individual experiment is shown here. Plots for 3 replicates are shown in Supplementary Fig. 9b-e. (**c**) Strong single-cell correlations within biaxial plots indicate co-regulated phosphorylation sites. (**d**) Unchanged and reduced correlations indicate unrelated phosphorylation sites. (**e**) and (**f**) Heat maps showing for all pairs of measured markers the change in Fisher-transformed Spearman correlation values for overexpression of (**e**) $KRAS^{G12V}$-GFP and (**f**) $MEK1^{DD}$-GFP when compared to the FLAG-GFP overexpression control. (**g**) and (**h**) BP-R^2 scores and Spearman correlations of bin medians for all measured markers in cells where (**g**) $KRAS^{G12V}$-GFP or (**h**) $MEK1^{DD}$-GFP was overexpressed overlaid on a literature-based graph of canonical signaling pathways14,15,21,23,44,45,35,46–48. Strong relationships identified from the BP-R^2 analysis are plotted on the signaling maps as colored circles. The sizes of circles indicate relationship strengths quantified by BP-R^2. The directionalities of relationships, as judged by Spearman correlation of bin medians, are shown by the color of the circles (positive correlation indicates that cells show generally increasing marker levels, and a negative correlation indicates decreasing marker levels as POI-GFP levels increase). For (e) to (h), data from 3 individual experiment replicates were used.

Europe PMC Funders Author Manuscripts

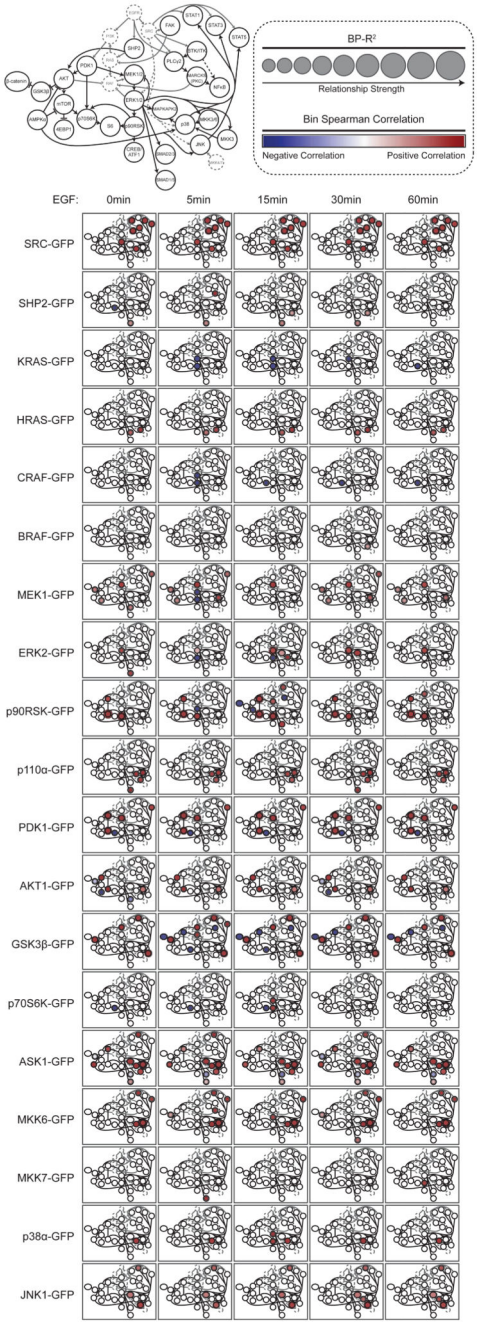

Figure 3.

Analysis of dynamics of EGFR signaling. HEK293T cells overexpressing GFP-tagged signaling proteins listed in Table 1 were treated with EGF for 0, 5, 15, 30, and 60 min. Strong abundance-dependent signaling relationships (Supplementary Fig. 10c) are plotted on the signaling map with circle sizes and colors indicating strengths (BP-R^2 score) and directionalities (Spearman correlation of bin medians), respectively. The miniaturized network is the same as used in Fig. 2. Overexpression of S6-GFP did not induce any strong

signaling relationships (data not shown). For all analyses, data from 3 individual experiment replicates were used.

Europe PMC Funders Author Manuscripts

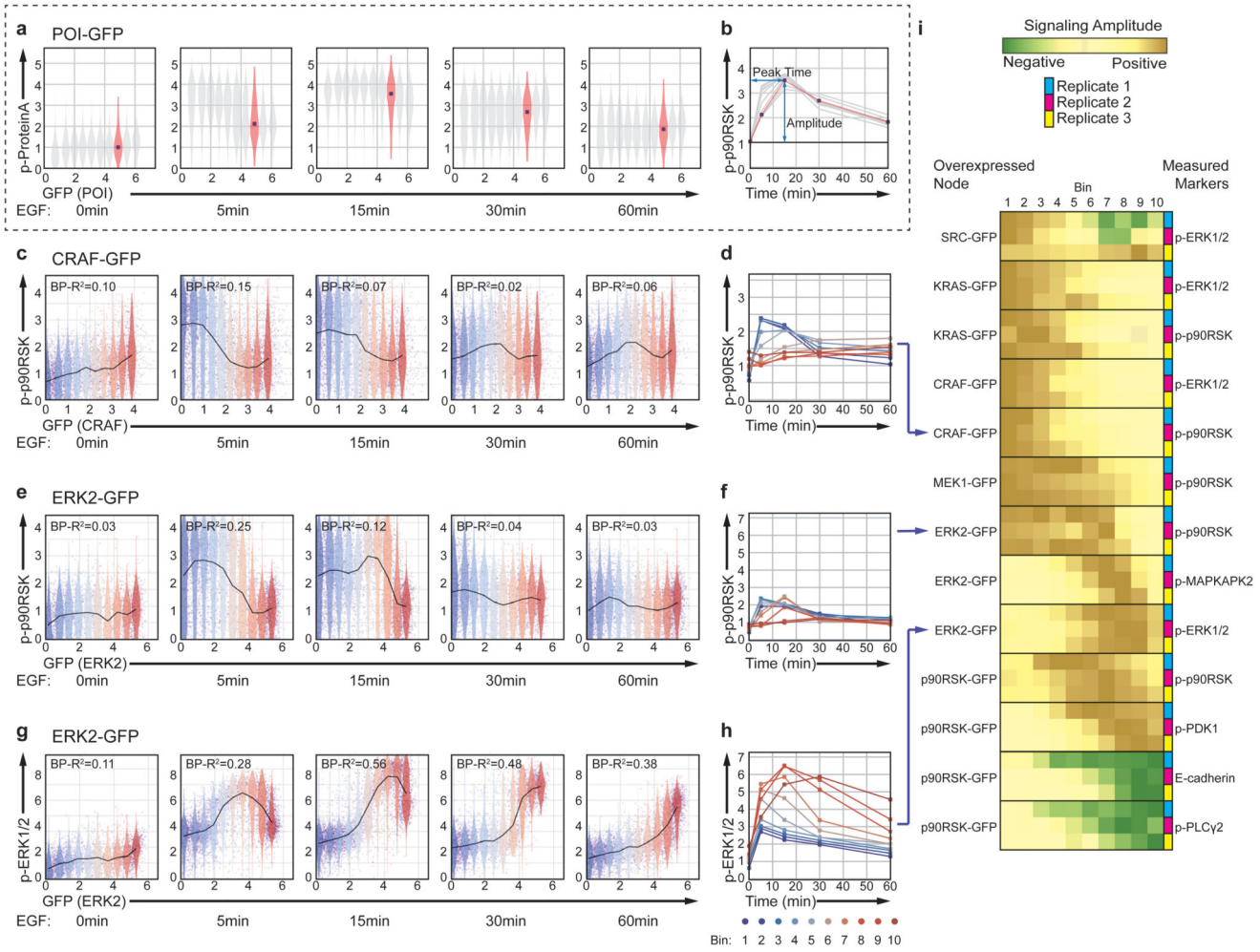

Figure 4.

Analysis of node abundance-dependent EGFR signaling dynamics. (**a, b**) Schematic plots of amplitude and peak-time analysis. (**a**) The x-axis (i.e., overexpressed protein as determined by the GFP measurement) was split into 10 bins. (**b**) Median phosphorylation abundance in each bin was plotted on the y-axis versus time (x-axis) to visualize abundance dependency of signaling dynamics. (**c, d**) Mass cytometry ion counts (arcsinh transformed, Methods) measured for p-p90RSK (y-axis) as a function of ion counts measured for abundance of CRAF-GFP (x-axis) and EGF stimulation time. The same layouts for (**e, f**) ERK2-GFP abundance-determined p-p90RSK levels and (**g, h**) p-ERK1/2 levels are shown. (**i**) Heat map showing protein abundances with strong influences on signaling amplitudes with color indicating normalized signaling amplitudes. Only overexpressed proteins with an amplitude-ratio higher than 3 fold for more than two of the three replicates were identified as strong influences and are included in the heat map. For (a) to (h), representative examples from the 3 individual experiment replicates are shown. Other replicates are presented in Supplementary File 5. In (i), all replicate data are shown.

Europe PMC Funders Author Manuscripts

Europe PMC Funders Author Manuscripts

Table 1

Overexpressed signaling proteins

Overexpressed proteins	Gene ID	UniProt Entry
SRC	*SRC*	P12931
PDK1	*PDPK1*	O15530
AKT1	*AKT1*	P31749
GSK3β	*GSK3B*	P49841
MKK7	*MAP2K7*	O14733
MKK6	*MAP2K6*	P52564
p38α	*MAPK14*	Q16539
ERK2	*MAPK1*	P28482
p90RSK	*RPS6KA1*	Q15418
CRAF	*RAF1*	P04049
JNK1	*MAPK8*	P45983
p110α	*PIK3CA*	P42336
BRAF	*BRAF*	P15056
ASK1	*MAP3K5*	Q99683
p70S6K	*RPS6KB1*	P23443
MEK1	*MAP2K1*	Q02750
KRAS	*KRAS*	P01116
HRAS	*HRAS*	P01112
SHP2	*PTPN11*	Q06124
S6	*RPS6*	P62753

Europe PMC Funders Author Manuscripts

Table 2

Relationships with shortest singed directed path length above 3 in the SIGNOR database

Overexpressed POI	Target	Sign	Shortest Signed Directed Path (SIGNOR)	Literature Information
SRC	p-BTK/ITK	1	6	SRC family kinases phosphorylate BTK48
SHP2	p-S6	-1	5	Known regulation49
ASK1	p-PDK1	1	5	Potential novel relationship
SRC	p-PLCγ2	1	5	SRC family kinases activates PLCγ248
ASK1	p-AMPKα	1	4	Potential novel relationship
GSK3β	p-SHP2	1	4	Potential novel relationship
p90RSK	p-PDK1	1	4	Potential novel relationship
JNK1	p-STAT1	1	4	JNK activates STAT150
JNK1	p-MAPKAPK2	1	4	Potential novel relationship
p110α	p-MKK3/6	1	4	Potential novel relationships
HRAS	p-SMAD2/3	1	4	Known crosstalk21
ASK1	p-GSK3β	1	4	Potential novel relationships
PDK1	p-S6	-1	4	Overexpression-induced negative regulation
p70S6K	p-S6	-1	4	Overexpression-induced negative regulation